BIOCHEMISTRY
including biophysical chemistry & molecular biology

Article

pubs.acs.org/biochemistry

The Functional Property Changes of Muscular $Na_v1.4$ and Cardiac $Na_v1.5$ Induced by Scorpion Toxin BmK AGP-SYPU1 Mutants Y42F and Y5F

Xiangxue Meng,[†,§] Yijia Xu,[†] Mingyi Zhao,*[,†] Fangyang Wang,[†] Yuanyuan Ma,[†] Yao Jin,[†] Yanfeng Liu,[†] Yongbo Song,[†] and Jinghai Zhang*[,†,‡,§]

[†]School of Life Sciences & Biopharmaceutical Science, Shenyang Pharmaceutical University, 103 Wenhua Road, 110016 Shenyang, PR China

[‡]School of Medical Devices, Shenyang Pharmaceutical University, 103 Wenhua Road, 110016 Shenyang, PR China

[§]Benxi Medicine Institute, Shenyang Pharmaceutical University, Shiqiaozi, 177005 Benxi, PR China

Supporting Information

ABSTRACT: Scorpion toxins are invaluable therapeutic leads and pharmacological tools which influence the voltage-gated sodium channels. However, the details were still unclear about the structure−function relationship of scorpion toxins on VGSC subtypes. In the previous study, we reported one α-type scorpion toxin Bmk AGP-SYPU1 and its two mutants (Y5F and Y42F) which had been demonstrated to ease pain in mice acetic acid writhing test. However, the function of Bmk AGP-SYPU1 on VGSCs is still unknown. In this study, we examined the effects of BmK AGP-SYPU1 and its two mutants (Y5F and Y42F) on $hNa_v1.4$ and $hNa_v1.5$ heterologously expressed CHO cell lines by using Na^+-specialized fluorescent dye and whole-cell patch clamp. The data showed that BmK AGP-SYPU1 displayed as an activator of $hNa_v1.4$ and $hNa_v1.5$, which might indeed contribute to its biotoxicity to muscular and cardiac system and exhibited the functional properties of both the α-type and β-type scorpion toxin. Notably, Y5F mutant exhibited lower activatory effects on $hNa_v1.4$ and $hNa_v1.5$ compared with BmK AGP-SYPU1. Y42F was an enhanced activator and confirmed that the conserved Tyr42 was the key amino acid involved in bioactivity or biotoxicity. These data provided a deep insight into the structure−function relationship of BmK AGP-SYPU1, which may be the guidance for engineering α-toxin with high selectivity on VGSC subtypes.

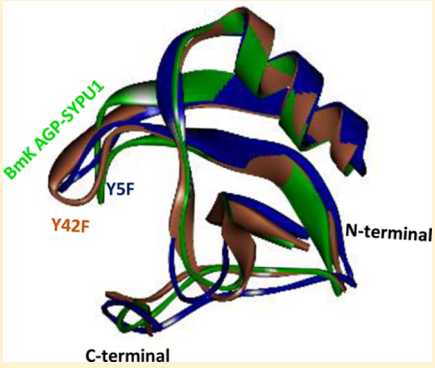

Many long-chain toxins purified from *Buthus martensii* Karsch (BmK) scorpion venom have been proved the diversity of bioactivity. These toxins can be classified into α-type (site 3) and β-type scorpion toxins (site 4) according to their binding preferences to the receptor sites of voltage-gated sodium channel (VGSCs).[1] α-Type long-chain scorpion toxin can prolong the action potentials of excitable cells *in vivo* by targeting VGSCs and kill organisms by inducing paralysis and arrhythmia.[2]

To date, the essential role of VGSCs has been emphasized in pathogenesis of acute and chronic pain,[3] epilepsy,[4] and cardiopathy.[5−7] $Na_v1.4$ and $Na_v1.5$ exhibit highly limited expression in skeletal and cardiac muscle cells, respectively. Genetic defects in the *SCN4A* gene are associated with hypokalemic periodic paralysis (HypoPP), hyperkalemic periodic paralysis (HyperPP), paramyotonia congenita (PMC), and potassium-aggravated myotonia (PAM).[8−11] Defects in *SCN5A* gene are associated with long QT syndrome type 3 (LQT3),[5−7] Brugada syndrome,[12−14] and primary cardiac conduction disease.[15] Most of these missense mutations have drawn much attention because the defects in $Na_v1.4$ and $Na_v1.5$ inactivation will cause small sustained sodium currents after the action potential explosion, ultimately resulting in devastating consequences. Same consequences could also be induced by α-type long-chain scorpion toxin, which could slow or block the inactivation and prolong the action potentials of excitable cells *in vivo* by targeting VGSCs.

On the basis of the previous data, it can be summarized that there are mainly three function-related domains in α-type scorpion toxins, which include the N-terminal domain comprises (the first three N-terminal residues), the Core-domain (the loop preceding the α-helix and the other loop between the β2- and β3-sheets), and the NC-domain (8−12 residues turn) (Figure 1).[16] Furthermore, some regions or residues, such as site RC,[17] cysteine (or disulfide bridges),[18,19] and conserved aromatic residues, have been proved to be associated with the bioactivity of α-type scorpion toxins. The conserved hydrophobic surface (CHS) has been proved conserved in all scorpion toxin structures known, which was mainly constituted by Tyr5, Tyr35, and Trp/Tyr47. The CHS

Received: January 24, 2015
Revised: April 27, 2015
Published: April 28, 2015

DOI: 10.1021/acs.biochem.5b00067
Biochemistry 2015, 54, 2988−2996

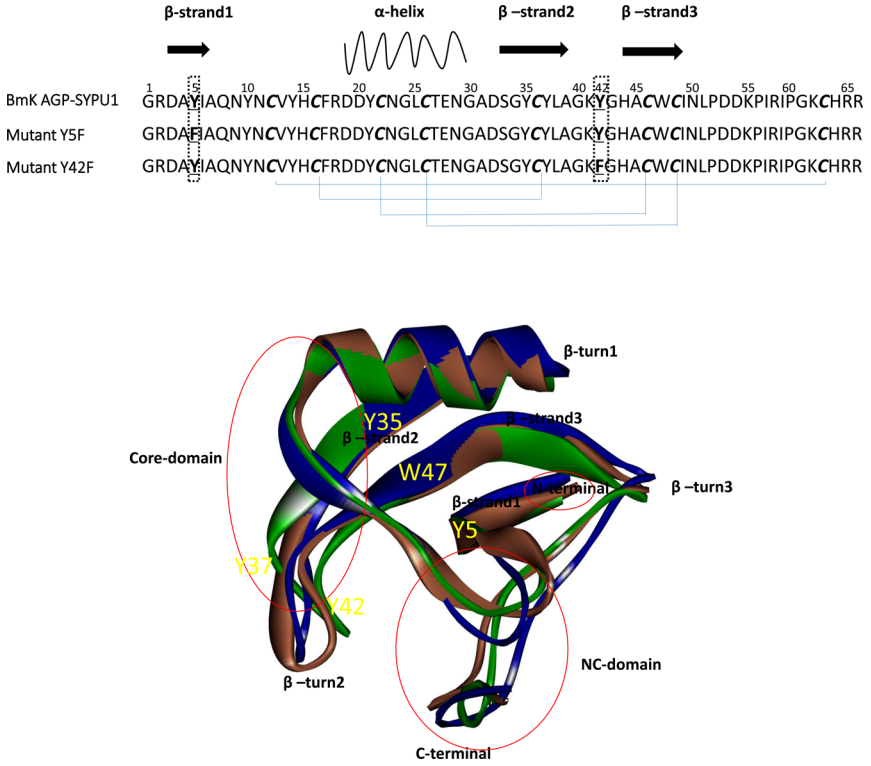

Figure 1. Comparison of the refined BmK AGP-SYPU1 model with its mutations Y42F and Y5F. Secondary structures and the sequence alignment between three toxins. The final stable 3D structure of BmK AGP-SYPU1 (green), Y42F (brown), and Y5F (deep-blue) (modeled by Deng et al.[22]). The secondary structural elements are composed of β-strands and α-helix (Y/F 5 and Y/F 42 labeled in black box, the conserved aromatic residue labeled with yellow, and the disulfide bonds were labeled with blue lines). The Core-domain, NC-domain and N-terminal are labeled with red circles. The conserved aromatic (Y5, Y35, Y37, Y42, W47) residues also labeled out in 3D structure.

and each of aromatic residues in it were proposed to be responsible for the bioactivity.[2] It also has been reported that the conserved Tyr5, Tyr35, and Trp47 were important to the structure and function of BmKM1, whereas Tyr42 and Trp38 were most likely involved in its bioactivity.[20]

Our group has been engaged in exploring new peptides from the Chinese scorpion *Buthus martensii* Karsch and pursuing to elucidate the essential association of their structures with the bioactivity for decades. BmK AGP-SYPU1 (*GU726488*) is purified from the Chinese scorpion *Buthus martensii* Karsch and has been identified as α-like type scorpion toxin according to the bioinformation analysis.[21] The residues Tyr5 and Tyr42 are highly conserved in long-chain scorpion toxins and contribute to the stability of Core-domain in molecular modeling.[22] The 3D structure of BmK AGP-SYPU1 revealed that Tyr5 and Tyr42 were located relatively close to each other and might form the aromatic cluster with other tyrosines and tryptophans to stabilize the structure of the native toxin[17] (Figure 1). These information indicates that the residue Tyr5 and Tyr42 in BmK AGP-SYPU1 may be related to bioactivity, then a certain number of mutants were produced. Finally, two mutants (Y5F and Y42F) of BmK AGP-SYPU1 drew our attention due to their much higher analgesic activity compared to the wild-type peptide in mice acetic acid writhing test.[22] The comparison of 3D structure between BmK AGP-SYPU1 and two mutants (Y42F and Y5F) was showed in Figure 1.

In this study, a series of experiments were conducted to clarify the effects of Bmk AGP-SYPU1 on $hNa_v1.4$ and $hNa_v1.5$ and the role of Tyr5 and Tyr42 in Bmk AGP-SYPU1. The initial functional properties of BmK AGP-SYPU1 and two mutants (Y5F and Y42F) on $hNa_v1.4$ and $hNa_v1.5$ were evaluated by using sodium influx measurement and whole-cell patch clamp. The evidence presented in this study would to the further understanding about the relationship of scorpion structure with its potential function on muscular and cardiac system.

2. MATERIALS AND METHODS

2.1. Materials. IMDM, 0.25% trypsin−EDTA, FBS, HT supplement, GlutaMAX. The sodium-sensitive dye SBFI-AM (sodium-binding benzofuran isophthalate) and Pluronic F127 were obtained from Life Technology. G418 was purchased from Calbiochem.

BmK AGP-SYPU1 and two mutants (Y5F and Y42F) were prepared as previously described.[18,22] Briefly, the pSYPU/1b-toxin expression vector was transformed into *Escherichia coli* BL21 (DE3). The bacteria cells grew in temporate conditions, and the supernatant containing recombinant toxin was harvested. The recombinant BmK AGP-SYPU1 and two mutants were purified by Nickel metal chelating ion affinity chromatography, followed by a cation exchange chromatography subsequently. All purified toxins were analyzed by SDS-PAGE (data not shown) and diluted in Lock's buffer and external solution for Na^+ influx experiment and the whole-cell patch clamp, respectively.

2.2. Cell Culture. CHO cells were cultured in IMDM with 2 mM GlutaMAX and supplemented with 100 μM hypoxanthine, 16 μM thymidine, and 10% FBS. $hNa_v1.4$-CHO and $hNa_v1.5$-CHO cells were cultured in IMDM with 2 mM GlutaMAX and supplemented with 100 μM hypoxanthine, 16 μM thymidine, 10% FBS, and 200 μg/mL G418. All cells

DOI: 10.1021/acs.biochem.5b00067
Biochemistry 2015, 54, 2988−2996

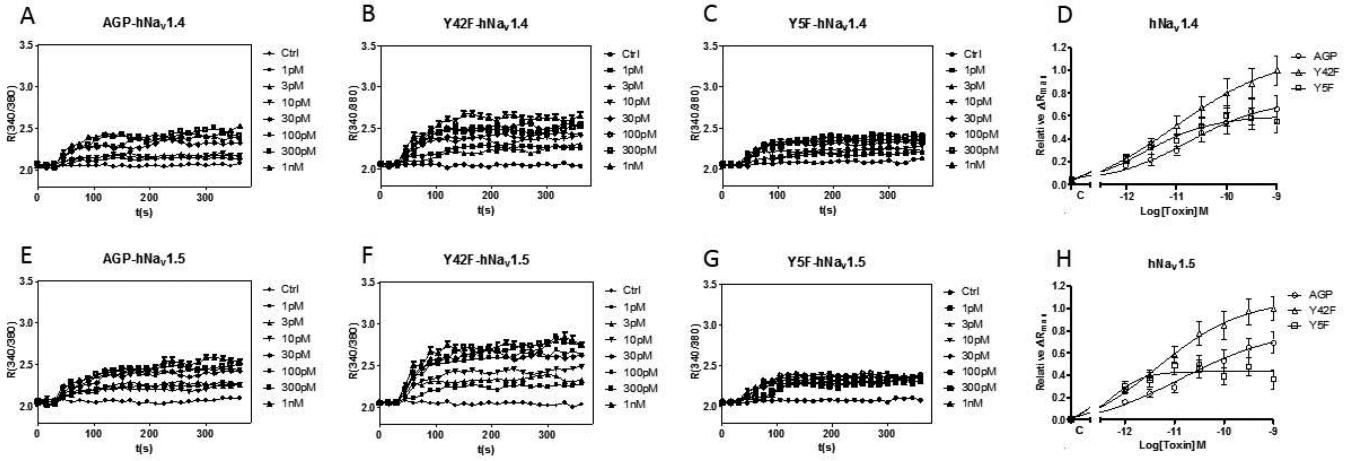

Figure 2. Time−response relationships for BmK AGP-SYPU1 stimulation of sodium influx in CHO cells heterologously expressing $hNa_v1.4$ (A) and $hNa_v1.5$ (E). Time−response relationships for Y42F stimulation of sodium influx in CHO cells heterologously expressing $hNa_v1.4$ (B) and $hNa_v1.5$ (F). Time−response relationships for Y5F stimulation of sodium influx in CHO cells heterologously expressing $hNa_v1.4$ (C) and $hNa_v1.5$ (G). Each data point represents the mean ± SEM of five determinations. Concentration−relative ΔR_{Max} relationships for BmK AGP-SYPU1, Y42F, and Y5F stimulation of sodium influx in heterologously expressing $hNa_v1.4$ (D) and $hNa_v1.5$ (H). Each data point represents the mean ± SEM of six determinations.

were cultured routinely as monolayers on poly-D-lysine coated dishes in an atmosphere of 5% CO_2 and 37 °C.

2.3. Sodium (Na^+) Influx Measurement and Data Analysis. *2.3.1. Sodium (Na^+) Influx Measurement.* The cells were collected after treated with 0.25% trypsin−EDTA for 3 min and washed four times with Lock's buffer (in mM: 5.6 KCl, 154 NaCl, 5.6 glucose, 1.0 $MgCl_2$, 2.3 $CaCl_2$, 0.1 glycine, 8.6 Hepes/NaOH, pH 7.4). The background fluorescence of each well in the 384-well, clear-bottomed black well plates (Nunc) was measured and averaged prior to detection. Cells were harvested after centrifugation and then incubated for 1 h at 25 °C with dye loading buffer (5×10^6 cells/mL) containing 10 μM SBFI-AM and 0.02% Pluronic F-127. After 1 h incubation in dye loading medium, cells were washed four times with Lock's buffer, diluted to a final concentration of 5×10^6 cells/mL in a final volume of 25 μL in each well. The plate was then transferred to the plate chamber of a Tecan infinite M200pro (TECAN, Swiss). Cells were excited at 340 and 380 nm and Na^+ bound SBFI emission were detected at 505 nm. Fluorescences were read were taken every 5 s up to total 45 s to establish the baseline, and then 5 μL of peptide containing solution (6×) was added to each well plate at the rate of 100 μL/s from the compound, yielding a final volume of 30 μL/well. The cells were exposed to the peptide for another 315 s. The raw emission data at 340 and 380 nm excitation wavelengths were exported to an Excel work sheet and corrected by the background fluorescence.

2.3.2. Data Analysis. The SBFI fluorescence ratios (340/380) versus time were analyzed, and the data reading was recorded as R_{base} and R_{max} before and after exposure to peptides. The maximal increment of SBFI fluorescence ratio was calculated with $\Delta R_{Max} = R_{max} - R_{base}$. The maximum response values for scorpion toxins were determined by nonlinear regression analysis using a logistic equation. In this experiments, the differences in normalized SBFI fluorescence ratios were analyzed by one-way ANOVA.[23]

2.4. Automated Patch-Clamp Electrophysiology Recording and Data Analysis. *2.4.1. Electrophysiology Recording.* Whole-cell patch clamp recording was used to examine functional properties of $hNa_v1.4$-CHO and $hNa_v1.5$-CHO cell lines using an automated electrophysiology platform (NPC-1 and Port-a-Patch system, Nanion Technologies GmbH, Munich, Germany) and an EPC10 amplifier (HEKA Elektronik, Lambrecht, Germany). Cells were detached with 0.25% trypsin−EDTA, terminated in fresh culture medium, centrifuged (100*g*, 3 min) and resuspended in external solution to reach a density of 1×10^6 cells/mL. Patchcontrol HT software (Nanion Technologies GmbH, Germany) was used to control application of solutions and pressures necessary to establish the whole-cell configuration. Sodium currents were recorded at room temperature (20−25 °C) using external (in mM: 140 NaCl, 4 KCl, 1 $MgCl_2$, 2 $CaCl_2$, 5 D-glucose monohydrate, 10 HEPES/NaOH, pH 7.4) and internal solutions (in mM: 50 CsCl, 10 NaCl, 60 CsF, 20 EGTA, 10 HEPES/CsOH, pH 7.2) identical to those used for conventional patch clamp experiments. Following cells contact with the 2−3.5 MΩ planar electrode, seal enhancer solution (in mM: 80 NaCl, 3 KCl, 35 $CaCl_2$, 10 $MgCl_2$, 10 HEPES/NaOH, pH 7.4) was added to the external solution to promote GΩ seal formation. After the whole-cell configuration was established, the seal enhancer solution was replaced with two washes of fresh external solution and the series resistance was compensated automatically. Patchmaster software (HEKA Elektronik, Lambrecht, Germany) was used to automatically compensate for whole cell capacitance and series resistance and to perform voltage-clamp protocols. Whole-cell currents were low-pass filtered at 5 kHz and digitized at 50 kHz.[24]

2.4.2. Data Analysis. The holding potentials were −80 mV. The Na^+ currents (I) were elicited by test pulses ranging from −80 to +80 mV for 50 ms with increments of 10 mV. The amplitudes of transient sodium currents (I_c and I) were recorded before and after the applications of different concentration BmK AGP-SYPU1. $\Delta I/I_c = (I - I_c)/I_c$ was used to determine the increment of peak current induced by BmK AGP-SYPU1. G/G_{max} was used to determine the voltage dependence of activation, the sodium conductance was calculated using $G = I(V_m - V_r)$, where V_r was reversal potential. G value for each test potential was normalized to G_{max} and plotted against the test potential to produce a voltage dependence of activation curves, which were fitted using

DOI: 10.1021/acs.biochem.5b00067
Biochemistry 2015, 54, 2988−2996

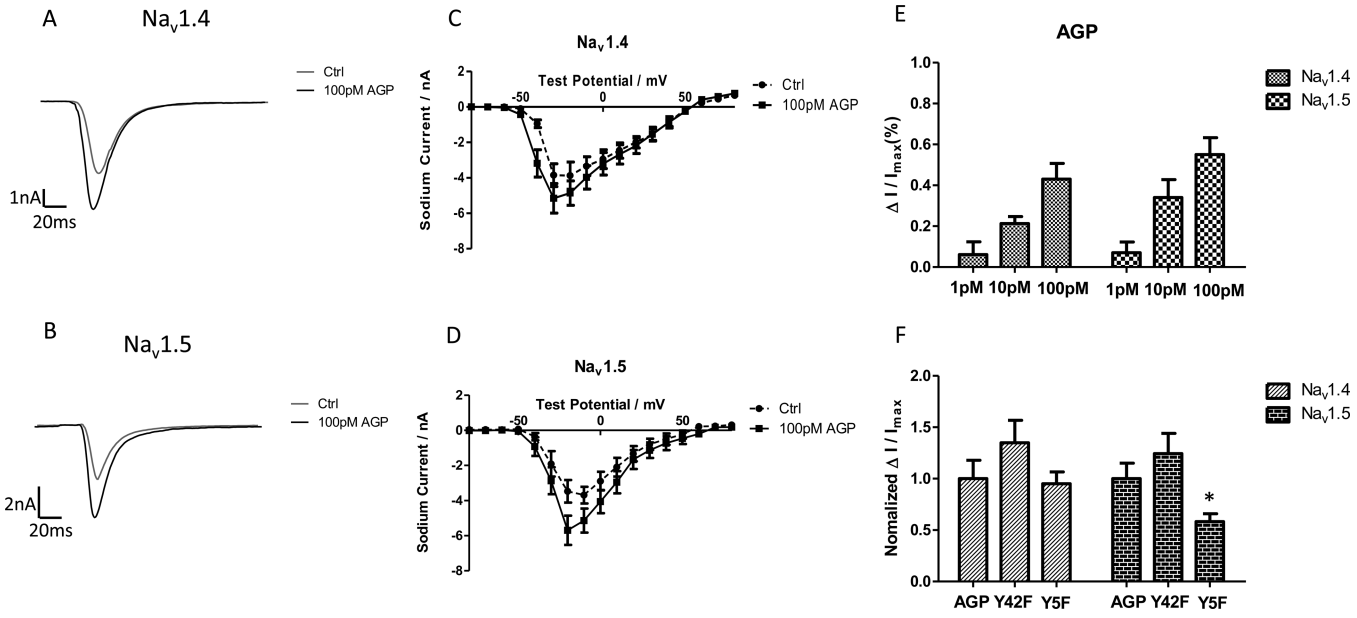

Figure 3. Effects of BmK AGP-SYPU1 and two mutants (Y42F and Y5F) on the Na^+ peak current of hNa$_v$1.4 and hNa$_v$1.5. The current traces evoked by −30 mV (hNa$_v$1.4) and −20 mV (hNa$_v$1.5) for 50 ms from a holding potential of −80 mV in the absence and presence of 100 pM BmK AGP-SYPU1. Averaged current traces obtained from hNa$_v$1.4-CHO (A) and hNa$_v$1.5-CHO (B) cells in each group. Statistical plots of the $I-V$ relationship of hNa$_v$1.4 (C) and hNa$_v$1.5 (D) after application of 100 pM BmK AGP-SYPU1.The Na^+ currents obtained by plotting current peak amplitudes with a function of test potentials ranging from −80 to +80 mV for 50 ms from the holding potential of −80 mV in increments of 10 mV. Normalized Na^+ peak current increment ratio ($\Delta I/I_c$) depolarized at −30 mV (hNa$_v$1.4) and −20 mV (hNa$_v$1.5) after 5 min treatment in absence and presence of 1, 10, and 100 pM BmK AGP-SYPU1 (E). Normalized $\Delta I/I_c$ to BmK AGP-SYPU1 depolarized at −30 mV (hNa$_v$1.4) and −20 mV (hNa$_v$1.5) evoked by 100 pM mutants from hNa$_v$1.4 and hNa$_v$1.5 (F). *P < 0.05, significant difference between BmK AGP-SYPU1 and Y5F values, **P < 0.01, significant difference between Y42F and Y5F values; paired one-way ANOVA. Each data point represents mean ± SEM for at least five experiments for each concentration.

Boltzmann functions: $G/G_{max} = 1/\{1 + \exp[(V_m - V_{1/2})/k]\}$, where $V_{1/2}$ was the voltage where half-maximal activation occurred, and k was a slope factor. Steady-state inactivation curves were fitted with the Boltzmann equations: $I/I_{max} = 1/\{1 + \exp[(V_m - V_{1/2})/k]\}$. I/I_{max} was normalized current. $V_{1/2}$ was the potential for half-maximal inactivation, and k was the slope factor of the fit. The time course of recovery of the Na^+ currents from inactivation was fitted with a tertiary exponential functions: $I/I_{max} = A\{1 - \exp[-\Delta t/\tau]\}$, where I_{max} was the maximal current amplitude, I was the current after a recovery period of Δt, τ was the time constant for recovery from inactivation, and A was the amplitude coefficient. The data was presented as mean ± SEM. Statistical analysis was carried out using one-way ANOVA. *P < 0.05 and ** P < 0.01 were considered to be statistically significant.

3. RESULTS

3.1. BmK AGP-SYPU1 and Two Mutants (Y42F and Y5F) Produced Sodium Influx on CHO Cell Lines Heterologously Expressing hNa$_v$1.4 and hNa$_v$1.5. The influence of BmK AGP-SYPU1 in sodium influx was examined by using fluorescence detection in order to demonstrate a consequence of activation of hNa$_v$1.4 and hNa$_v$1.5 subunits due to exposure to the toxins. BmK AGP-SYPU1 produced a minimal sodium influx in CHO cells as control (Supporting Information, Figure 1). As shown in Figure 2, BmK AGP-SYPU1 and two mutants (Y42F and Y5F) produced a rapid elevation of sodium influx in a concentration-dependent manner in hNa$_v$1.4-CHO and hNa$_v$1.5-CHO cell lines, respectively. There was a significant reduction of the efficiency of Y5F on hNa$_v$1.5 and no evident decrement of efficiency on hNa$_v$1.4 compared with BmK AGP-SYPU1, suggesting a softly weakened activatory effect of Y5F on hNa$_v$1.5. However, Y42F appeared to activate both hNa$_v$1.4 and hNa$_v$1.5, which were approximately 1.5-fold more potent than BmK AGP-SYPU1.

3.2. Effects of BmK AGP-SYPU1 and Two Mutants (Y42F and Y5F) on the Amplitude of Sodium Current Evoked from hNa$_v$1.4 and hNa$_v$1.5. BmK AGP-SYPU1 was tested at increasing concentrations (1, 10, and 100 pM). The current traces were evoked in absence and presence of BmK AGP-SYPU1 at a dose of 100 pM (Figure 3A,B). The inward sodium currents were evoked during depolarization with an increment interval of 10 mV from −80 to 80 mV and the peak current appeared at voltages between −30 and −20 mV (Figure 3C,D). As shown in Figure 3E, BmK AGP-SYPU1 increased the amplitude of sodium current in a concentration-dependent manner, with a statistically significant increment at 100 pM. The maximal increase of peak amplitude induced by BmK AGP-SYPU1 was 43 ± 7.6% and 55 ± 8.3% on hNa$_v$1.4 and hNa$_v$1.5 respectively. The results indicated that BmK AGP-SYPU1 could enhance the activation of hNa$_v$1.4 and hNa$_v$1.5, which was consistent with other α-like type scorpion toxins. To evaluate the potency changes of the toxins after the amino acid alteration, the increment ratio of peak current induced by 100 pM of Y42F and Y5F were shown (control for 100%) in Figure 3F. Y42F induced a slightly stronger sodium current (1.2−1.3-fold) than BmK AGP-SYPU1 from both hNa$_v$1.4 and hNa$_v$1.5, although the enhancement exhibited no statistical significance. Y5F attenuated the increment of peak current evoked from both hNa$_v$1.4 and hNa$_v$1.5 in comparison with BmK AGP-SYPU1, although the statistically attention only could be seen in hNa$_v$1.5. The distinct effects on enhancing the amplitude of

DOI: 10.1021/acs.biochem.5b00067
Biochemistry 2015, 54, 2988−2996

sodium current caused by mutants seemed consistent with the results in Na^+ influx detection experiment. It suggested that Y42F was stronger to activate the $hNa_v1.4$ and $hNa_v1.5$, while Y5F was weaker compared to BmK AGP-SYPU1.

3.3. Effects of BmK AGP-SYPU1 Mutant Y42F on Functional Properties of $hNa_v1.4$ and $hNa_v1.5$. The effects of 100 pM of BmK AGP-SYPU1 and Y42F were determined and compared on channel properties of $hNa_v1.4$ and $hNa_v1.5$. After exposure to 100 pM of BmK AGP-SYPU1, the $I-V$ curve significantly shifted to the hyperpolarized orientation on $hNa_v1.4$ and $hNa_v1.5$ (Figure 3C,D), with the $V_{1/2}$ of activation decreased by −4.6 and −3.9 mV, respectively (Table 1). 100 pM of Y42F shifted the $V_{1/2}$ of activation by −3.7 mV ($hNa_v1.4$) and −6.4 mV ($hNa_v1.5$), compared with control value (Figure 4A,B). The slowing inactivation of $hNa_v1.4$ was enhanced by Y42F compared with BmK AGP-SYPU1, while that of $hNa_v1.5$ was weakened (Figure 4C,D). Generally speaking, the recovery duration of $hNa_v1.4$ and $hNa_v1.5$ from inactivation were delayed after exposure to Y42F at a dose of 100 pM (Figure 5A,B). The activation and inactivation parameters were summarized in Table 1. The slope factors against control almost kept unchanged.

3.4. Effects of BmK AGP-SYPU1 Mutant Y5F on Functional Properties of $hNa_v1.4$ and $hNa_v1.5$. Nevertheless, the effects changes of Y5F seemed exactly different from those of Y42F. Y5F took no significant action on the $V_{1/2}$ values of activation for both $hNa_v1.4$ and $hNa_v1.5$ in comparison with control (Figure 4,B). Both BmK AGP-SYPU1 and Y5F shifted inactivation of $hNa_v1.4$ and $hNa_v1.5$ to the depolarizing direction (Figure 4C,D). Referring to $hNa_v1.4$, Y5F significantly increased the $V_{1/2}$ value of inactivation by 6.8 mV, whereas BmK AGP-SYPU1 only increased $V_{1/2}$ value slightly by 1.6 mV (Table 1). It might be the major reason why Y5F did not alter the sodium current amplitude of $hNa_v1.4$ compared with BmK AGP-SYPU1. Notably, the time course of recovery induced by Y5F was longer than that of BmK AGP-SYPU1 on $hNa_v1.4$ (Figure 5A). These appearances might due to the affinity increment between Y5F and $hNa_v1.4$. The affinity increment might have no direct equivalence to functional property modifications. Y5F also induced a significantly slowing inactivation of $hNa_v1.5$, although the performance was much weaker than BmK AGP-SYPU1. The recovery course induced by Y5F from inactivation to the rest state was much faster than that induced by BmK AGP-SYPU1 (Figure 5B). The time course of recovery parameters are listed in Table 1. No slope factors of inactivation curves were affected after application of toxins.

4. DISCUSSION

Previous work has reported that the VGSCs activators shifted the VGSC activation voltage to the more negative value and inhibited inactivation of VGSCs, resulting in an increased Na^+ permeability of cells and enhancing the excitability of cells.[23] In this study, both the detection of Na^+ influx and the amplitude of sodium current suggested that BmK AGP-SYPU1 was a $hNa_v1.4$ and $hNa_v1.5$ activator. Several other α-type scorpion toxins with high similarity (DNA sequence similarity >70%) to BmK AGP-SYPU1 (including Lqq 3, Bot IT1 and BmK M1) have been characterized fully in previous study. Lqq 3 is high homologous (78% DNA sequence similarity) to BmK AGP-SYPU1, and the first α-type scorpion toxin is to be characterized highly toxic to mice [LD_{50} = 0.05 ng (7.1 pmol)/g body weight] by subcutaneous injection and [LD_{50} =

Table 1. Effects of BmK AGP-SYPU1 and Two Mutants (Y42F and Y5F) on the Kinetic Properties of $hNa_v1.4$ and $hNa_v1.5$

	$hNa_v1.4$				$hNa_v1.5$			
group	Ctrl	AGP	Y42F	Y5F	Ctrl	AGP	Y42F	Y5F
activation $V_{1/2}$ (mV)	−34.4 ± 0.85	−39 ± 0.94*[a]	−37.74 ± 1.03*[a]	−35.85 ± 1.14	−25.26 ± 0.65	−29.18 ± 0.98*[a]	−31.64 ± 1.09*[a]	−27.78 ± 0.95
k	6.58 ± 0.74	6.45 ± 0.64	7.34 ± 0.61	5.91 ± 0.83	7.33 ± 0.93	5.79 ± 0.75	6.73 ± 0.72	7.25 ± 0.69
inactivation $V_{1/2}$ (mV)	−38.58 ± 0.93	−37.02 ± 0.88	−34.93 ± 0.97*[a]	−32.64 ± 0.81*[a]	−39.51 ± 0.90	−32.70 ± 1.09*[a]	−37.63 ± 0.98	−35.49 ± 1.02*[a]
k	14.43 ± 1.07	13.52 ± 1.11	13.57 ± 1.04	13.20 ± 0.92	13.73 ± 0.93	12.97 ± 1.12	14.10 ± 1.09	13.82 ± 0.94
recovery τ (ms)	7.68 ± 1.08	9.85 ± 0.95	15.54 ± 0.84*[a]	11.94 ± 0.94*[a]	3.88 ± 1.42	9.39 ± 0.97*[a]	11.06 ± 0.87**[b]	7.78 ± 1.03*[a]

[a]*$P < 0.05$: significant difference between control and toxins on $hNa_v1.4$ and $hNa_v1.5$; one-way ANOVA. [b]**$P < 0.01$: significant difference between control and toxins on $hNa_v1.4$ and $hNa_v1.5$; one-way ANOVA.

DOI: 10.1021/acs.biochem.5b00067
Biochemistry 2015, 54, 2988−2996

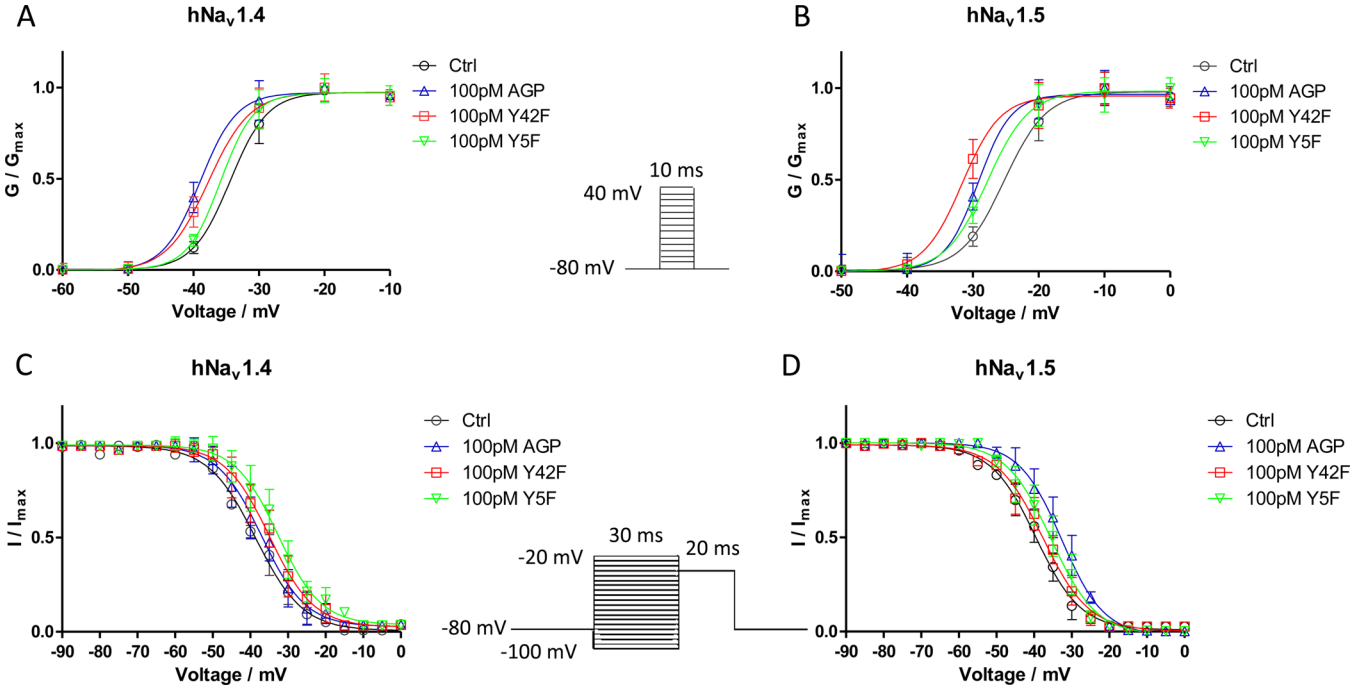

Figure 4. Effect of BmK AGP-SYPU1 and two mutants (Y42F and Y5F) on activation and inactivation kinetics of hNa$_v$1.4 and hNa$_v$1.5. Na^+ current was generated by applying pulses from −80 to +40 mV at 10 mV steps for 20 ms from. Peak current was converted into conductance, and normalized conductance of sodium channel is plotted against the voltages of conditioning pulses. The steady-state activation curves of hNa$_v$1.4 (A) and hNa$_v$1.5 (B). Each point represents mean ± SEM (n = 8). The currents were elicited with a test pulse at −20 mV for 20 ms following 30 ms prepulses ranging from −100 to −20 mV at 5 mV steps. Peak currents were normalized and the steady-state inactivation curves of hNa$_v$1.4 (C) and hNa$_v$1.5 (D) plotted against the command potentials. Each point represents mean ± SEM (n = 7).

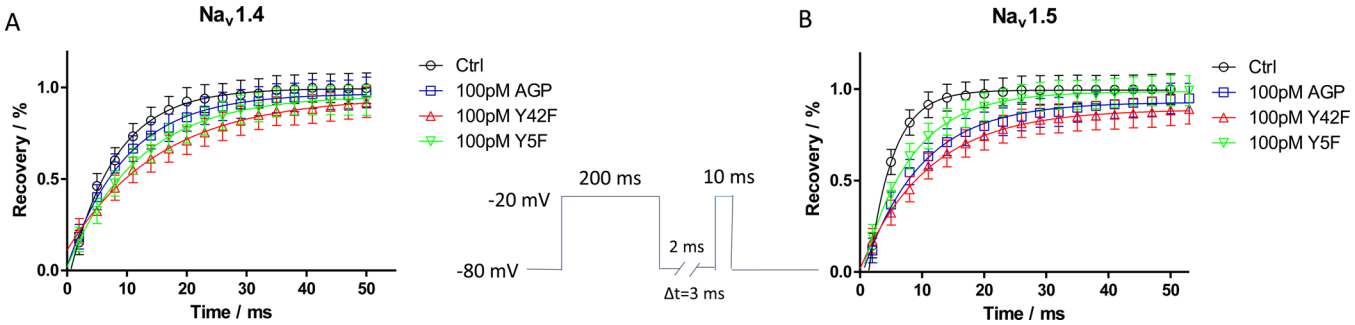

Figure 5. Effect of BmK AGP-SYPU1 and two mutants (Y42F and Y5F) on recovery from inactivation of Na^+ current. The currents were obtained at two-pulse, consisting of a 200 ms prepulse to −20 mV followed by resting at −80 mV for the time varying from 2 to 53 ms in increments of 3 ms and a test pulse to −20 mV for 10 ms. The ratio of I to I_{max} represented the recovery of Na^+ current from inactivation for hNa$_v$1.4 (A) and hNa$_v$1.5 (B). Each point represents mean ± SEM (n = 6).

0.055 ng (8 pmol)/g body weight] via the intracerebroventricular route.[25] Moreover, Lqq 3 exhibited an blockage effect of fast inactivation with the EC_{50} value of <2.5 nM on hNa$_v$1.5 expressed in HEK 293 cells.[26] In contrast, 100 pM of BmK AGP-SYPU1 enhanced the excitability of hNa$_v$1.4 and hNa$_v$1.5 markedly, indicating higher sensitivity to hNa$_v$1.4 and hNa$_v$1.5 than Lqq3. It is probably that BmK AGP-SYPU1 exhibits its biotoxicity by driving the excitable cells into higher exciting state and preventing the subsequent excitability transmission in skeletal and cardiac muscle cells, which definitely cause the paralysis in muscle and arrhythmias in heart. Consequently, BmK AGP-SYPU1 would be an important component in scorpion venom that killed organisms by inducing paralysis and arrhythmia.

Interestingly, despite of the definition of BmK AGP-SYPU1 as α-type scorpion toxin by bioinformation, BmK AGP-SYPU1 induced changes of both activation and inactivation property of VGSCs, exhibiting the interaction with both the site 3 and site 4 on VGSCs. The exact site of VGSCs interacting directly with BmK AGP-SYPU1 seems different from classical sites and might overlap the structural components involved in site 3 and site 4.[1] Coincidently, the existence of this phenomenon was not singular. The β-type scorpion toxins (including Css IV,[27,28] AaH IT4,[29] BmK AS,[28] and BmK AS-1[30]) and α-type scorpion toxin OD1[31] also displayed the functional properties of both the α-type and β-type scorpion toxins. The unique way of these scorpion toxins interacting with VGSCs might depend on their extraordinary structure. Unfortunately, the structure of these toxins has not been verified yet. Moreover, BmK AGP-SYPU1 exerted an inconsistent action on activation and inactivation kinetics between hNa$_v$1.4 and hNa$_v$1.5, indicating that the preference of BmK AGP-SYPU1 to site 3 or site 4 was also

DOI: 10.1021/acs.biochem.5b00067
Biochemistry 2015, 54, 2988−2996

relate to the fundamental diversity of VGSCs. These cross-type scorpion toxins enrich the varieties of scorpion toxins nowadays and might act as completely distinct probes for functional studies on VGSCs.

In a previous study, BmK AGP-SYPU1 displayed analgesic activity in acetic acid writhing test in mice. However, it showed activatory effect on $hNa_v1.4$ and $hNa_v1.5$ in vitro in this study. It seemed inconsistent between these two aspects. However, most of scorpion neurotoxins influenced various ion channels or different channel isoforms (sodium channel, potassium channel, and calcium channel). For instance, BmK AGAP (BmK antitumor-analgesic peptide) has been defined as the α-type scorpion toxin by bioinformation. Recently, BmK AGAP has been reported to serve as an analgesic by inhibiting calcium currents through N-, L-, and T-type channels in dorsal root ganglia (DRG) neurons.[32] Additionally, a couple of scorpion toxins display enormous functional properties on various subtypes of VGSCs. Such as BmK AS, BmK AS is a β-like scorpion toxin and displays the antinociceptive effect in rat models due to its remarkably suppressive effects on tetrodotoxin-resistant (TTX-R) and tetrodotoxin-sensitive (TTX-S) sodium current rat DRG neurons.[33] Nevertheless, the amplitude of sodium current increased and the recovery kinetics slowed, coupling with the action potential decayed after the application of BmK AS on $rNa_v1.2$.[28] On the basis of these researches, it is reasonable to propose the antinociceptive effect of BmK AGP-SYPU1 might involve other channels, such as voltage-gated calcium channel and other subtypes of VGSCs. Subsequent researches should be carried out to evaluate the potential analgesic mechanisms of BmK AGP-SYPU1, including the bioactivity or biotoxicity of BmK AGP-SYPU1 in vivo and the functional property changes induced by BmK AGP-SYPU1 on targets involved in pain-associated signal transduction pathway.

Molecular dissection of α-toxin involved in the interaction with the VGSCs receptor site 3 revealed a common bipartite bioactive surface, including one cluster of bioactive residues named Core-domain (Figure 1). A number of works have stated portions of information about the role of Core-domain in α-type scorpion. The Core-domain may be involved in the interaction with Gating-module of DIV on VGSCs and toxin potency on $rNa_v1.2a$.[34,35] As shown in Figure 6, The hydroxyl O of Tyr42 and Tyr5 formed hydrogen bonds with Pro60 and Lys41, respectively.[22] The formation of the hydrogen bonds were essential for stabilizing the conformation of the core domain.[22] After the Tyr42 or Tyr5 was substituted by phenylalanine, the hydrogen bond was removed and the angle of β-turn2 was altered significantly (Figure 1), resulting in the stability change of Core-domain. In this study, Y42F strengthened the activatory effect in $hNa_v1.4$ and $hNa_v1.5$ compared with BmK AGP-SYPU1. The biotoxicity of Y42F on muscular and cardiac system may be enhanced too. The results confirm that Tyr42 is related to the bioactivity, and the increment of biotoxicity can be achieved by weakening the stability of Core-domain after the alteration in Tyr42.

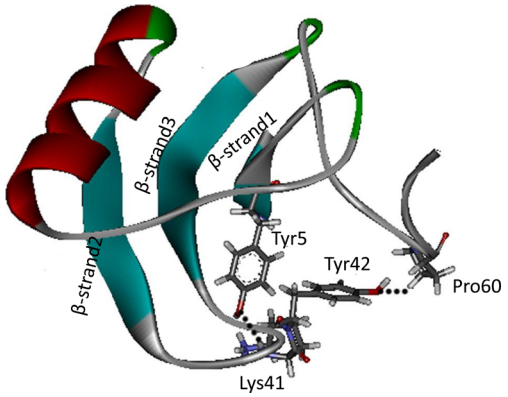

Figure 6. Two hydrogen bonds (one dotted line between Tyr5 and Lys 41, the other one for Tyr42 and Pro60) in the 3D structure of BmK AGP-SYPU1 (modeled by Deng et al.[22]). They were related to the stability of Core-domain in α-type scorpion toxins.[22]

As a highly conserved aromatic residue in CHS region, Tyr5 was proposed to be responsible for the pharmacological effects in α-type scorpion toxins for decades.[36] In this study, Y5F appeared to be a weaker activator on $hNa_v1.4$ and $hNa_v1.5$ compared with BmK AGP-SYPU1, which indicated the biotoxicity might attenuate to muscular and cardiac system. Obviously, the structural modification of Y5F increased the hydrophobicity of CHS and damaged the stability of Core-domain, suggesting that the biotoxicity alteration was related to the stability of Core-domain as well as the hydrophobicity of CHS. Additionally, Y5F showed more potent analgesic activity in previous work. It seems that the alteration in Tyr5 is meaningful to develop the α-toxins as the analgesic drug with low biotoxicity to the muscular and cardiac system.

Moreover, Tyr42 is located in the loop connecting the β2- and β3-sheets, which is remarkably different in sequence and structure between α-type and β-type scorpion toxins.[17] This residue may affect the performance of scorpion toxins as α-type or β-type.[20] In this study, Y42F showed a complex site preferences to $hNa_v1.4$ and $hNa_v1.5$. After the substitution of tyrosine by phenylalanine, the increment of hydrophobicity in this site was favorable for the site 3 preferences on $hNa_v1.4$, while the site 4 preferences on $hNa_v1.5$. On the whole, it seems that the preference to site 3 or site 4 is not only related to the key amino acid and the domain in toxins, but also the isoforms of VGSCs.

In conclusion, we demonstrated that BmK AGP-SYPU1 and two mutants (Y5F and Y42F) displayed as activators of $hNa_v1.4$ and $hNa_v1.5$. The effects on activation and inactivation induced by BmK AGP-SYPU1 indicated that it might exhibit the functional properties of both the α-type and β-type scorpion toxins. The results suggest that the conserved Tyr42 and Tyr5 are the key amino acids involved in bioactivity and biotoxicity of the toxin. These findings may facilitate the structural modification of other α-type scorpion toxins to achieve the high preference to their bioactivity target with lower side effects.

■ ASSOCIATED CONTENT

Ⓢ Supporting Information

Time−response relationships for BmK AGP-SYPU1 stimulation of sodium influx in CHO cell. The Supporting Information is available free of charge on the ACS Publications website at DOI: 10.1021/acs.biochem.5b00067.

■ AUTHOR INFORMATION

Corresponding Authors

*For J.H.Z.: phone, +86-024-23986431; fax, +86-024-23986431; E-mail, zhangjinghai@syphu.edu.cn .
*For M.Y.Z.: phone, +86-024-23986431; fax, +86-024-23986431; E-mail, zmy_dl@126.com.

DOI: 10.1021/acs.biochem.5b00067
Biochemistry 2015, 54, 2988−2996

Funding
We gratefully acknowledge financial support from the National Key Scientific Project for New Drug Discovery and Development of China (no. 2014ZX09101044-001), National Natural Science Foundation of China (no. 30931872), and National Natural Science Foundation of China (no. 81102365).

Notes
The authors declare no competing financial interest.

■ ABBREVIATIONS USED
BmK, *Buthus martensii* Karsch; Lqq, *Leiurus quinquestriatus* quinquestriatus; Bot, *Buthus occitanus* tunetanus; Css, *Centruroides suffusus* suffuses; AaH, *Androctonus australis* Hector; OD, *Odontobuthus doriae*; SBFI, sodium-binding benzofuran isophthalate; VGSC, voltage-gated sodium channel; CHS, conserved hydrophobic surface; DRG, dorsal root ganglia; TTX-R, tetrodotoxin-resistant; TTX-S, tetrodotoxin-sensitive

■ REFERENCES
(1) Catterall, W. A., Cestele, S., Yarov-Yarovoy, V., Yu, F. H., Konoki, K., and Scheuer, T. (2007) Voltage-gated ion channels and gating modifier toxins. *Toxicon 49*, 124−141.
(2) Bosmans, F., and Tytgat, J. (2007) Voltage-gated sodium channel modulation by scorpion alpha-toxins. *Toxicon 49*, 142−158.
(3) Woolf, C. J., and Ma, Q. (2007) Nociceptors—noxious stimulus detectors. *Neuron 55*, 353−364.
(4) Catterall, W. A. (2014) Sodium channels, inherited epilepsy, and antiepileptic drugs. *Annu. Rev. Pharmacol. Toxicol. 54*, 317−338.
(5) Wang, Q., Shen, J., Splawski, I., Atkinson, D., Li, Z., Robinson, J. L., Moss, A. J., Towbin, J. A., and Keating, M. T. (1995) SCN5A mutations associated with an inherited cardiac arrhythmia, long QT syndrome. *Cell 80*, 805−811.
(6) Ruan, Y., Liu, N., and Priori, S. G. (2009) Sodium channel mutations and arrhythmias. *Nature Rev. Cardiol. 6*, 337−348.
(7) Ruan, Y., Liu, N., Bloise, R., Napolitano, C., and Priori, S. G. (2007) Gating properties of SCN5A mutations and the response to mexiletine in long-QT syndrome type 3 patients. *Circulation 116*, 1137−1144.
(8) George, A. L., Jr. (2005) Inherited disorders of voltage-gated sodium channels. *J. Clin. Invest. 115*, 1990−1999.
(9) Cannon, S. C. (2002) An expanding view for the molecular basis of familial periodic paralysis. *Neuromuscular Disord. 12*, 533−543.
(10) Lehmann-Horn, F., and Jurkat-Rott, K. (1999) Voltage-gated ion channels and hereditary disease. *Physiol. Rev. 79*, 1317−1372.
(11) Jurkat-Rott, K., and Lehmann-Horn, F. (2001) Human muscle voltage-gated ion channels and hereditary disease. *Curr. Opin. Pharmacol. 1*, 280−287.
(12) Chen, Q., Kirsch, G. E., Zhang, D., Brugada, R., Brugada, J., Brugada, P., Potenza, D., Moya, A., Borggrefe, M., Breithardt, G., Ortiz-Lopez, R., Wang, Z., Antzelevitch, C., O'Brien, R. E., Schulze-Bahr, E., Keating, M. T., Towbin, J. A., and Wang, Q. (1998) Genetic basis and molecular mechanism for idiopathic ventricular fibrillation. *Nature 392*, 293−296.
(13) Hedley, P. L., Jorgensen, P., Schlamowitz, S., Moolman-Smook, J., Kanters, J. K., Corfield, V. A., and Christiansen, M. (2009) The genetic basis of Brugada syndrome: a mutation update. *Human Mutat. 30*, 1256−1266.
(14) Marquez, M. F., Bonny, A., Hernandez-Castillo, E., De Sisti, A., Gomez-Flores, J., Nava, S., Hidden-Lucet, F., Iturralde, P., Cardenas, M., and Tonet, J. (2012) Long-term efficacy of low doses of quinidine on malignant arrhythmias in Brugada syndrome with an implantable cardioverter-defibrillator: a case series and literature review. *Heart Rhythm 9*, 1995−2000.
(15) Royer, A., van Veen, T. A., Le Bouter, S., Marionneau, C., Griol-Charhbili, V., Leoni, A. L., Steenman, M., van Rijen, H. V., Demolombe, S., Goddard, C. A., Richer, C., Escoubet, B., Jarry-Guichard, T., Colledge, W. H., Gros, D., de Bakker, J. M., Grace, A. A., Escande, D., and Charpentier, F. (2005) Mouse model of SCN5A-linked hereditary Lenegre's disease: age-related conduction slowing and myocardial fibrosis. *Circulation 111*, 1738−1746.
(16) Karbat, I., Frolow, F., Froy, O., Gilles, N., Cohen, L., Turkov, M., Gordon, D., and Gurevitz, M. (2004) Molecular basis of the high insecticidal potency of scorpion alpha-toxins. *J. Biol. Chem. 279*, 31679−31686.
(17) He, X. L., Li, H. M., Zeng, Z. H., Liu, X. Q., Wang, M., and Wang, D. C. (1999) Crystal structures of two alpha-like scorpion toxins: non-proline cis peptide bonds and implications for new binding site selectivity on the sodium channel. *J. Mol. Biol. 292*, 125−135.
(18) Ma, R., Cui, Y., Zhou, Y., Bao, Y. M., Yang, W. Y., Liu, Y. F., Wu, C. F., and Zhang, J. H. (2010) Location of the analgesic domain in Scorpion toxin BmK AGAP by mutagenesis of disulfide bridges. *Biochem. Biophys. Res. Commun. 394*, 330−334.
(19) Sun, Y. M., Liu, W., Zhu, R. H., Goudet, C., Tytgat, J., and Wang, D. C. (2002) Roles of disulfide bridges in scorpion toxin BmK M1 analyzed by mutagenesis. *J. Pept. Res. 60*, 247−256.
(20) Sun, Y. M., Bosmans, F., Zhu, R. H., Goudet, C., Xiong, Y. M., Tytgat, J., and Wang, D. C. (2003) Importance of the conserved aromatic residues in the scorpion alpha-like toxin BmK M1: the hydrophobic surface region revisited. *J. Biol. Chem. 278*, 24125−24131.
(21) Wang, Y., Wang, L., Cui, Y., Song, Y. B., Liu, Y. F., Zhang, R., Wu, C. F., and Zhang, J. H. (2010) Purification, characterization and functional expression of a new peptide with an analgesic effect from Chinese scorpion *Buthus martensii* Karsch (BmK AGP-SYPU1). *Biomed. Chromatogr. 25*, 801−807.
(22) Deng, L., Zhang, H. X., Wang, Y., Zhang, R., Wen, X., Song, Y. B., Zhao, Y. S., Ma, L., Wu, C. F., and Zhang, J. H. (2014) Site-directed mutagenesis of BmK AGP-SYPU1: the role of two conserved Tyr (Tyr5 and Tyr42) in analgesic activity. *Protein J. 33*, 157−164.
(23) Cao, Z., George, J., Gerwick, W. H., Baden, D. G., Rainier, J. D., and Murray, T. F. (2008) Influence of lipid-soluble gating modifier toxins on sodium influx in neocortical neurons. *J. Pharmacol. Exp. Ther. 326*, 604−613.
(24) Kahlig, K. M., Lepist, I., Leung, K., Rajamani, S., and George, A. L. (2010) Ranolazine selectively blocks persistent current evoked by epilepsy-associated Nanu1.1 mutations. *Br. J. Pharmacol. 161*, 1414−1426.
(25) Kopeyan, C., Mansuelle, P., Martin-Eauclaire, M. F., Rochat, H., and Miranda, F. (1993) Characterization of toxin III of the scorpion *Leiurus quinquestriatus quinquestriatus*: a new type of alpha-toxin highly toxic both to mammals and insects. *Natural Toxins 1*, 308−312.
(26) Chen, H., and Heinemann, S. H. (2001) Interaction of scorpion alpha-toxins with cardiac sodium channels: binding properties and enhancement of slow inactivation. *J. Gen. Physiol. 117*, 505−518.
(27) Thomsen, W., Martin-Eauclaire, M. F., Rochat, H., and Catterall, W. A. (1995) Reconstitution of high-affinity binding of a beta-scorpion toxin to neurotoxin receptor site 4 on purified sodium channels. *J. Neurochem. 65*, 1358−1364.
(28) Zhu, M. M., Tao, J., Tan, M., Yang, H. T., and Ji, Y. H. (2009) U-shaped dose-dependent effects of BmK AS, a unique scorpion polypeptide toxin, on voltage-gated sodium channels. *Br. J. Pharmacol. 158*, 1895−1903.
(29) Loret, E. P., Martin-Eauclaire, M. F., Mansuelle, P., Sampieri, F., Granier, C., and Rochat, H. (1991) An anti-insect toxin purified from the scorpion *Androctonus australis* Hector also acts on the alpha- and beta-sites of the mammalian sodium channel: sequence and circular dichroism study. *Biochemistry 30*, 633−640.
(30) Jia, L. Y., Zhang, J. W., and Ji, Y. H. (1999) Biosensor binding assay of BmK AS-1, a novel Na+ channel-blocking scorpion ligand on rat brain synaptosomes. *Neuroreport 10*, 3359−3362.
(31) Durek, T., Vetter, I., Wang, C. I., Motin, L., Knapp, O., Adams, D. J., Lewis, R. J., and Alewood, P. F. (2013) Chemical engineering and structural and pharmacological characterization of the alpha-scorpion toxin OD1. *ACS Chem. Biol. 8*, 1215−1222.
(32) Liu, X., Li, C., Chen, J., Du, J., Zhang, J., Li, G., Jin, X., and Wu, C. (2014) AGAP, a new recombinant neurotoxic polypeptide, targets

DOI: 10.1021/acs.biochem.5b00067
Biochemistry 2015, 54, 2988−2996

the voltage-gated calcium channels in rat small diameter DRG neurons. *Biochem. Biophys. Res. Commun. 452*, 60−65.
(33) Chen, J., Tan, Z. Y., Zhao, R., Feng, X. H., Shi, J., and Ji, Y. H. (2005) The modulation effects of BmK I, an alpha-like scorpion neurotoxin, on voltage-gated Na(+) currents in rat dorsal root ganglion neurons. *Neurosci. Lett. 390*, 66−71.
(34) Gurevitz, M. (2012) Mapping of scorpion toxin receptor sites at voltage-gated sodium channels. *Toxicon 60*, 502−511.
(35) Kahn, R., Karbat, I., Ilan, N., Cohen, L., Sokolov, S., Catterall, W. A., Gordon, D., and Gurevitz, M. (2009) Molecular requirements for recognition of brain voltage-gated sodium channels by scorpion alpha-toxins. *J. Biol. Chem. 284*, 20684−20691.
(36) Kharrat, R., Darbon, H., Rochat, H., and Granier, C. (1989) Structure/activity relationships of scorpion alpha-toxins. Multiple residues contribute to the interaction with receptors. *Eur. J. Biochem. 181*, 381−390.

DOI: 10.1021/acs.biochem.5b00067
Biochemistry 2015, 54, 2988−2996